CONEM 2016
CONGRESSO NACIONAL DE ENGENHARIA MECÂNICA
21 - 25 AGOSTO DE 2016
FORTALEZA - CEARÁ

MULTI-OBJECTIVE OPTIMIZATION OF THE 1045 STEEL DRY END MILLING PROCESS BASED ON NORMAL BOUNDARY INTERSECTION AND PRINCIPAL COMPONENTS ANALYSIS

Gabriela Belinato, gabrielabelinato@gmail.com[1,2]
Danielle M Duarte Costa, danielle.costa@ifsuldeminas.edu.br[1,2]
Pedro Paulo Balestrassi, ppbalestrassi@gmail.com[1]
[1]Universidade Federal de Itajubá, Itajubá - MG
[2]Instituto Federal do Sul de Minas, Pouso Alegre – MG

Resumo: *This work introduces a mathematical approach that combine the Normal Boundary Intersection method with principal Components Analysis (NBI-PCA) for correlated responses.Theoretical results indicate that the solution found by NBI-PCA approach characterized as an appropriate optimal point. In this case, a cutting speed of 330.20 m/min, feed rate of 0.06 mm/tooth, axial depth of cut of 1.45 mm and radial depth of cut of 16.33 mm are the optimal cutting parameters for minimum roughness and maximum material removal rate. These results were validated statistically confirming the adequacy of the work's proposal.*

Keywords: *Dry end milling, Optimization, Principal Analysis Component, NormalBoundary Intersection.*

1. INTRODUCTION

In looking for the best process operating condition, the traditional experimental strategy is to analyze the behavior of some desired features that are considered significant as a function of the factor's increment (Paiva, 2007). However, as occur in most of the machining processes, and also in end milling, the multiple quality characteristics measured are highly correlated and with different optimization objectives (Patwari, 2008; Moshat et al., 2010; Thangarasu, 2012; Kumar, 2013; Singh, 2014; Kumar 2014; Singh et al., 2014; Bhogal, 2015). In this cases, the presence of correlation, or the use of optimization methods that do not consider it, can cause the model's instability, the overfitting, and the inaccuracy on the regression coefficients (Bratvhell, 1989; Chiao, 2011). In fact, if the influence of the correlation structure that exists in the original data set is ignored, one achieves an unreliable setting that improves the quality of all the responses simultaneously (Chiao, 2011; Wu, 2005). Furthermore, the individual analysis of each response may lead to a conflicting optimum, since the factor levels that improve one response can, otherwise, degrade another (Chiao, 2011).

In addressing the correlation influence in multi-objective optimization problems, researchers have used the Principal Component Analysis (PCA) as the principal approach (Tong, 2005; Murthy, 2012; De Freitas et al., 2012; Chen et al., 2015).

PCA is a multivariate analysis technique able to summarize, in a few uncorrelated components, common patterns of variation among response variables (Paiva, 2007; De Freitas et al., 2012; Antony, 2000).

According to Johnson and Wicher (Johnson, 2007), PCA uses the factorization of a variance-covariance $(\sum)$ or correlation (R) matrix associated with the random vector $Y^T = [Y_1, Y_2, ..., Y_p]$, to produce pairs of eigenvalues-eigenvectors $(\lambda_i, e_i),... \geq (\lambda_p, e_p)$ where $\lambda_1 \geq \lambda_2 \geq ... \geq \lambda_p \geq 0$ and an uncorrelated linear combination $PC_i = e_i^T Y = e_{1i}Y_1 + e_{2i}Y_2 + ... + e_{pi}Y_p$, $i = 1,2,..., p$. The original data set may be then replaced by the uncorrelated linear combinations in the form of principal components score (PC_{score}). PC_{score} can be written as $PC_{score} = [Z] \times [E]$, where Z is the standardized data matrix and E is the eigenvectors matrix of the multivariate set.

Using the Kaiser's criteria, only the principal components whose eigenvalues are greater than one, and whose explained cumulative variance are greater than 80% can be used to replace the original responses (Paiva et al., 2010).

The proposal of this work is a strategy for optimize a correlated multi-objective problems that combines PCA with Response Surface Methodology (RSM), obtain the uncorrelated objective functions represented by the scores of the PCA and apply the Normal Boundary Intersection method (NBI). When these methods are applied, it is possible to find Pareto optimal points that are the solutions for this kind of problems.

To illustrate this proposal, a case study of AISI 1045 steel end milling process is used. The optimization results will be validated statistically to confirm the adequacy of the work's proposal.

2. NORMAL BOUNDARY INTERSECTION METHOD

The Normal Boundary Intersection method was developed by Das and Dennis (1998) for finding a uniformly spread Pareto-optimal solutions for a general nonlinear multi-objective optimization problem. In this way, the NBI method is able to compensate the shortcomings attributed to the Weighted Sums method.

The establishment of payoff matrix $\overline{\mathbf{\Phi}}$ is the first step in the NBI method given by the calculation of the minimum $f_i^*\left(x_i^*\right)$ and maximum $f_i\left(x_i^*\right)$ values of the i-th objective function $f_i\left(x\right)$. The payoff matrix $\overline{\mathbf{\Phi}}$ can be written as:

$$\Phi = \begin{bmatrix} f_1^*\left(x_1^*\right) & \cdots & f_1\left(x_i^*\right) & \cdots & f_1\left(x_m^*\right) \\ \vdots & \ddots & & & \vdots \\ f_i\left(x_1^*\right) & \cdots & f_i^*\left(x_i^*\right) & \cdots & f_i\left(x_m^*\right) \\ \vdots & & & \ddots & \vdots \\ f_m\left(x_1^*\right) & \cdots & f_m\left(x_i^*\right) & \cdots & f_m^*\left(x_m^*\right) \end{bmatrix} \tag{1}$$

The objective functions can be normalized by using $f_i^*\left(x_i^*\right)$ and $f_i\left(x_i^*\right)$ values, mostly when different scales or units are used to define them. A vector with the set of individual minimum can be written such as $f^U = \left[f_1^*\left(x_1^*\right) \;\; \ldots, \;\; f_i^*\left(x_i^*\right) \;\; \ldots, \;\; f_m^*\left(x_m^*\right)\right]^T$, to obtain the Utopia point $f_i^*\left(x_i^*\right)$. This specific point is generally outside of the feasible region that corresponds to all objectives simultaneously being at their best possible values. The Nadir point $f_i\left(x_i^*\right)$, likewise, is obtained by joining the maximum values of each objective function $f^N = \left[f_1^N \;\; \ldots, \;\; f_i^N \;\; \ldots, \;\; f_m^N\right]^T$. It is the design space where all objectives are simultaneously at their worst values. When the i-th objective is minimized independently the two anchor points are obtained, and the Utopia line is the one that connects them.

The normalization of the objective functions can be obtained using these two sets, as in:

$$\bar{f}\left(x\right) = \frac{f_i\left(x\right) - f_i^U}{f_i^N - f_i^U}, i = 1, \ldots, m \tag{2}$$

This normalization leads to scalarization of the payoff matrix $\overline{\mathbf{\Phi}}$ and the vector $\overline{\mathbf{F}}\left(\mathbf{x}\right)$. Associated to vector of weights $\boldsymbol{\beta}$ and an unitary normal vector $\hat{\mathbf{n}}$, the classical NBI formulation can be described as:

$$\begin{aligned} & \underset{(\mathbf{x}, t)}{Max}\, D \\ & S.t: \; \overline{\mathbf{\Phi}}\boldsymbol{\beta} + D\hat{\mathbf{n}} = \overline{\mathbf{F}}\left(\mathbf{x}\right) \\ & \qquad \mathbf{x} \in \Omega \\ & \qquad g_j(x) \leq 0 \\ & \qquad h_j(x) \leq 0 \end{aligned}$$

3. EXPERIMENTAL PROCEDURE

3.1. Machine and cutting tool

The experiments were conducted on a Fadal, vertical machining center, model VMC-15, having a maximum power of 15kW and maximum rotation speed of 7,500 RPM (Fig. 1a). The tool overhang was 60 mm. The tool used was a positive end mill, code R390-025A25-11M with a 25 mm diameter, entering angle of $\chi_r - 90^o$, and a medium step with three inserts. Three rectangular inserts were used (Fig. 1b) with edge lengths of 11 mm each, code R390-11T308M-PMGC-1025. The tool material used was cemented carbide ISO P10 coated with TiCN and TiN by the PVD process. The coating hardness was around 3000 HV3 and the substrate hardness 1650HV3 with a grain size smaller than

1 μm. The surface roughness of the machined surface of workpiece was measured using a Mitutoyo portable roughness meter, model Surftest SJ 201, with a cut-off length of 0.25 mm (Fig. 1c).

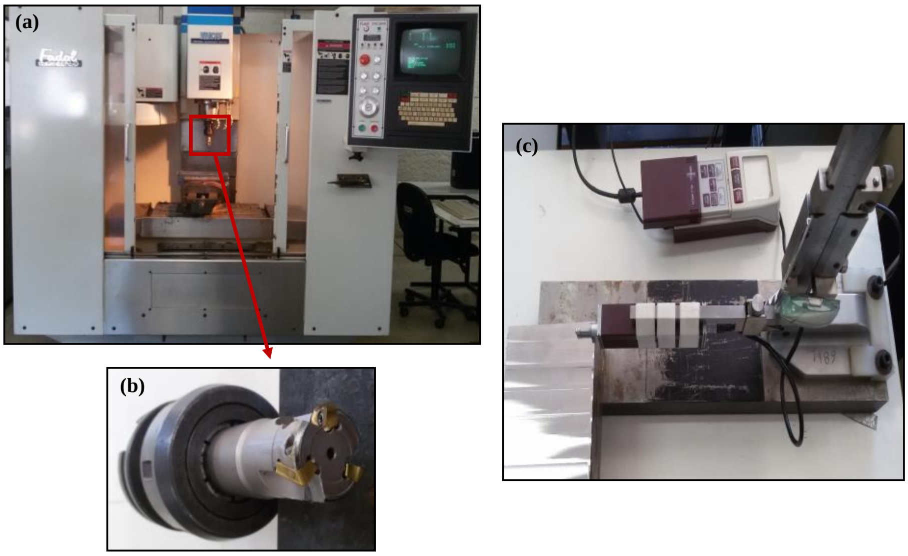

Figure 1. FADAL VMC (a), Rectangular inserts (b), Mitutoyo portable roughness (c).

3.2. Workpiece material

The workpiece material was AISI 1045 steel with a hardness of approximately 180 HB. The workpiece dimensions were rectangular blocks with square sections of 100x100 mm and lengths of 300 mm. The chemical composition of this steel includes the following: C (0.430-0.500%); Mn (0.600-0.900%); Pmax (0.040%) and Smax (0.050%).

3.3. Design of experiments and experimental results

The workpiece was machined using the range of parameters reported in Tab. 1. A Central Composite Design (CCD; Tab. 2) for four milling parameters at two levels, eight axial points and six center points was established. Six responses are analyzed: arithmetic average surface roughness (R_a), maximum surface roughness (R_y), root mean square roughness (R_q), ten point height (R_z), maximum peak to valley (R_t) and material removal rate (MRR). The experimental results were analyzed using statistical analysis with the help of software Minitab® 16.0.

Table 1. Cutting parameters and respective levels.

Cutting parameters	Levels (Uncoded and Coded)				
	-2	-1	0	+1	+2
Feed rate (f_z, mm/tooth)	0.05	0.10	0.15	0.20	0.25
Axial depth of cut (a_p, mm)	0.375	0.750	1.125	1.500	1.875
Cutting speed (V_c, m/min)	275	300	325	350	375
Radial depth of cut (a_e, mm)	13.5	15.0	16.5	18.0	19.5

Table 2. Experimental design

Exp. Nº	Cutting Parameters				Original responses						Principal Component Responses	
					Minimize					Maximized	Minimize	Maximized
	f_z	a_p	V_c	a_e	R_a	R_y	R_z	R_q	R_t	MRR	PC_1	PC_2
1	0.10	0.750	300	15.00	1.18	5.53	5.16	1.37	5.63	1.13	-2.18	-0.76
2	0.20	0.750	300	15.00	1.98	9.71	8.86	2.34	10.04	2.25	3.30	-1.30
3	0.10	1.500	300	15.00	1.17	5.01	4.76	1.36	5.14	2.25	-2.34	0.16
4	0.20	1.500	300	15.00	1.48	7.89	7.00	1.82	7.94	4.50	1.11	1.19
5	0.10	0.750	350	15.00	1.15	4.75	4.44	1.31	4.76	1.13	-2.92	-0.62

6	0.20	0.750	350	15.00	2.08	9.27	8.74	2.43	9.48	2.25	3.21	-1.36
7	0.10	1.500	350	15.00	1.10	5.06	4.62	1.25	5.16	2.25	-2.55	0.26
8	0.20	1.500	350	15.00	1.69	8.05	7.39	2.00	8.30	4.50	1.79	0.95
9	0.10	0.750	300	18.00	1.04	5.78	4.78	1.21	5.85	1.35	-2.44	-0.43
10	0.20	0.750	300	18.00	1.67	8.03	7.65	2.06	8.17	2.70	1.47	-0.46
11	0.10	1.500	300	18.00	1.16	5.22	4.95	1.34	5.38	2.70	-2.10	0.50
12	0.20	1.500	300	18.00	1.82	9.13	8.18	2.19	9.27	5.40	3.10	1.36
13	0.10	0.750	350	18.00	1.19	5.33	5.13	1.37	5.49	1.35	-2.22	-0.59
14	0.20	0.750	350	18.00	1.99	8.86	8.32	2.35	8.88	2.70	2.74	-0.87
15	0.10	1.500	350	18.00	1.18	5.13	4.79	1.36	5.35	2.70	-2.13	0.49
16	0.20	1.500	350	18.00	1.74	8.52	7.48	2.07	8.74	5.40	2.38	1.54
17	0.05	1.125	325	16.50	0.37	2.68	2.00	0.45	2.73	0.93	-6.52	0.35
18	0.25	1.125	325	16.50	1.86	9.12	8.71	2.26	9.28	4.64	3.20	0.69
19	0.15	0.375	325	16.50	1.54	6.69	5.99	1.75	6.84	0.93	-0.55	-1.42
20	0.15	1.875	325	16.50	1.16	6.13	5.47	1.39	6.20	4.64	-1.02	1.88
21	0.15	1.125	275	16.50	1.55	7.18	6.54	1.80	7.34	2.78	0.33	-0.09
22	0.15	1.125	375	16.50	1.61	7.25	6.83	1.87	7.52	2.78	0.62	-0.19
23	0.15	1.125	325	13.50	1.56	6.87	6.52	1.81	7.07	2.28	0.08	-0.47
24	0.15	1.125	325	19.50	1.60	7.09	6.72	1.85	7.49	3.29	0.61	0.23
25	0.15	1.125	325	16.50	1.57	6.90	6.48	1.82	7.10	2.78	0.22	-0.10
26	0.15	1.125	325	16.50	1.63	7.22	6.81	1.90	7.39	2.75	0.62	-0.23
27	0.15	1.125	325	16.50	1.66	7.35	6.90	1.94	7.43	2.72	0.76	-0.30
28	0.15	1.125	325	16.50	1.59	7.25	6.59	1.83	7.39	2.78	0.45	-0.14
29	0.15	1.125	325	16.50	1.61	7.18	6.70	1.87	7.33	2.78	0.52	-0.17
30	0.15	1.125	325	16.50	1.61	7.18	6.69	1.85	7.32	2.81	0.49	-0.14
Utopia Point (ζ_{y_j})					0.47	2.70	2.32	0.55	2.79	6.14	-6.20	2.35

4. RESULTS AND DISCUSSION

4.1. Modeling of the dry end milling process

Considering the aim to analyze the influence of the dry end milling cutting parameters on the six measured responses, the second-order polynomial models were developed using RSM. To estimate the coefficients, the Semiparametric Least Squares (SLS) algorithm was employed and the results are presented in Tab. 3.

Table 3. Quadratic models for responses and ANOVA

Coeficient	R_a	R_y	R_z	R_q	R_t	MRR	PC_1	PC_2
Constant	**1.612**	**7.180**	**6.694**	**1.869**	**7.326**	**2.770**	0.507	**-0.179**
f_z	**0.344**	**1.689**	**1.600**	**0.430**	**1.715**	**0.928**	**2.393**	**0.113**
a_p	**-0.071**	**-0.182**	**-0.206**	**-0.074**	**-0.179**	**0.928**	-0.110	**0.810**
V_c	0.031	-0.050	0.006	0.025	-0.037	0.000	0.040	-0.028
a_e	0.002	0.049	0.030	0.006	0.063	**0.253**	0.101	**0.185**
f_z^2	**-0.113**	**-0.265**	**-0.286**	**-0.113**	**-0.282**	0.004	**-0.472**	**0.155**
a_p^2	**-0.054**	-0.138	**-0.192**	**-0.059**	-0.153	0.004	**-0.254**	**0.083**
V_c^2	0.004	0.063	0.047	0.007	0.074	0.003	0.061	-0.010
a_e^2	0.004	0.005	0.030	0.006	0.037	0.004	0.030	-0.005
f_z x a_p	**-0.065**	-0.082	**-0.196**	**-0.072**	-0.101	**0.310**	-0.185	**0.326**
f_z x V_c	0.030	0.076	0.057	0.027	0.076	0.000	0.119	-0.038
f_z x a_e	0.001	-0.093	-0.064	0.006	-0.130	**0.085**	-0.051	**0.073**
a_p x V_c	-0.029	0.022	-0.049	-0.032	0.056	0.000	-0.059	0.032
a_p x a_e	**0.060**	**0.203**	**0.184**	**0.062**	**0.233**	**0.085**	**0.319**	-0.023
V_c x a_e	0.013	0.043	0.047	0.016	0.053	0.000	0.069	-0.020

Adj.R^2 (%)	93.84	92.78	94.32	95.11	92.94	99.93	95.24	97.56
Regression p-value	0.000	0.000	0.000	0.000	0.000	0.000	0.000	0.000
Normality (AD) test	0.309	0.509	0.327	0.261	0.550	1.614	0.536	0.416
Normality (AD) p-value	0.538	0.116	0.506	0.682	0.144	<5%	0.156	0.312
Curvature p-value	0.000	0.011	0.007	0.001	0.004	0.411	0.001	0.003

Note: Bold values represent the individually significant terms (p-value<5%).

4.2. Optimization by NBI

Of the six measured responses, all the roughness responses (R_a, R_y, R_q, R_z, R_t) present a strong and positive correlation, with significant statistic (Tab. 4). A moderate positive correlation among MRR in relation to roughness responses was observed.

Table 4. Correlation structure among responses.

	R_a	R_y	R_z	R_q	R_t
R_y	0.956 (0.000)				
R_z	0.976 (0.000)	0.991 (0.000)			
R_q	0. 996 (0.000)	0.972 (0.000)	0.989 (0.000)		
R_t	0.959 (0.000)	0.999 (0.000)	0.991 (0.000)	0.973 (0.000)	
MRR	0.457 (0.011)	0.579 (0.001)	0.549 (0.002)	0.499 (0.005)	0.578 (0.001)

As the responses of the dry end milling process are multi-correlated and considering that the objectives between these characteristics are conflicting (except the values of MRR, remaining responses need to be minimized), using PCA method to optimize is thus justified. Next, these components are optimized by Normal Boundary Intersection method to decide optimal factor levels.

The NBI-PCA approach is applied according the following steps.

4.2.1. Principal Component Analysis

Using the correlation matrix the principal components scores were extracted from the original responses and stored (Tab. 2) with their respective eigenvalues $\lambda_{PC\,i}$ and eigenvectors e_{ij} (Tab. 5). The first and second principal components are responsible for the explanation of 99.0% of the variation structure of the six dry end milling responses (Tab. 5). In this way, two uncorrelated objective functions formed by the first two principal components will be optimized through the NBI-PCA approach.

Table 5. Principal Component Analysis for dry end milling responses

Eigenvalue (λ_{ij})	5.254	0.683	0.054	0.007
Proportion	0.876	0.114	0.009	0.001
Cumulative	0.876	0.990	0.999	1.000
Eigenvectors (e_{ij})	PC_1	PC_2	PC_3	PC_4
R_a	0.424	-0.228	0.590	-0.393
R_y	0.433	-0.046	-0.495	-0.234
R_z	0.434	-0.101	-0.102	0.819
R_q	0.430	-0.174	0.393	0.129
R_t	0.433	-0.049	-0.467	-0.322
MRR	0.269	0.950	0.154	-0.012

As has been mentioned, the PCA obtains uncorrelated objective functions of principal components (0.000, p-value = 1.000).

4.2.2. RSM models for the significant principal components

Taking the scores calculated in the PCA and modeling them according to RSM, the following expressions were obtained:

$$\begin{aligned} PC_1 = {} & 0.507 + 2.393_{fz} - 0.110_{ap} + 0.040_{vc} + 0.101_{ae} - 0.472_{fz^2} - 0.254_{ap^2} + \\ & + 0.061_{vc^2} + 0.030_{ae^2} - 0.185_{fz*ap} + 0.119_{fz*vc} - 0.051_{fz*ae} - 0.059_{ap*vc} + \\ & + 0.319_{ap*ae} + 0.069_{\mathrm{vc*ae}} \end{aligned} \tag{4}$$

$$\begin{aligned} PC_2 = {} & -0.179 + 0.113_{fz} + 0.810_{ap} - 0.028_{vc} + 0.185_{ae} + 0.155_{fz^2} + 0.083_{ap^2} - \\ & - 0.010_{vc^2} - 0.005_{ae^2} + 0.326_{fz*ap} - 0.038_{fz*vc} + 0.073_{fz*ae} + 0.032_{ap*vc} - \\ & - 0.023_{ap*ae} - 0.020_{\mathrm{vc*ae}} \end{aligned} \tag{5}$$

Table 3 shows the ANOVA results for the identified PC models. For all of them, p-values less than 5% of significance. In relation to their adjustments, all of them presented an adj. R^2 of 97.18% for $PC_1$and for 98.64% for PC_2 and no lack of fit was observed. All curvature p-values presented a value lower than 5% of significance. Figure 4 shows the response surface graphics for analyzed characteristics.

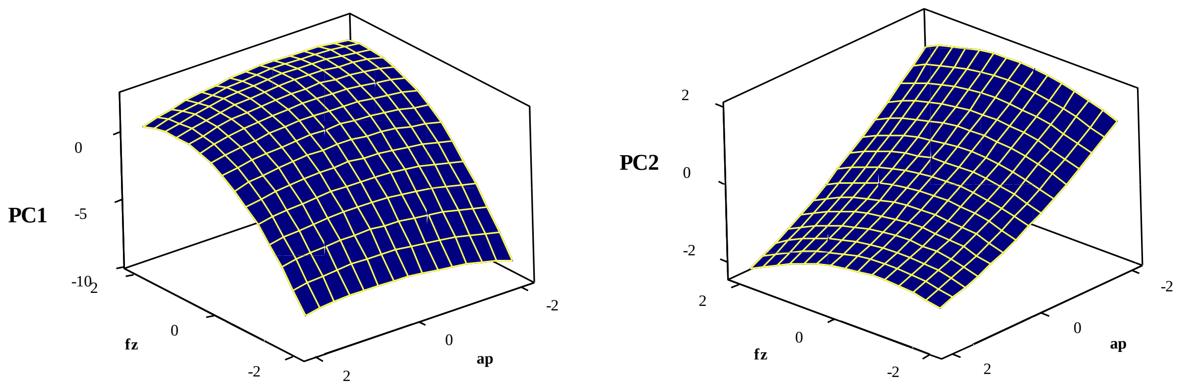

Figure 4. Response surfaces for PC_1 and PC_2

4.2.3. Constrained optimization of $\hat{y}_j$

The Utopia point (ζ_{y_j}) for the original responses and for the significant principal components were established by individual constraint minimization (for roughness responses and PC_1) and individual constraint maximization (for MRR response and PC_2), such as $\zeta_{y_i} = \underset{\mathbf{x}\in\Omega}{Min}\left[\hat{y}_j(\mathbf{x})\right]$ and $\zeta_{y_i} = \underset{\mathbf{x}\in\Omega}{Max}\left[\hat{y}_j(\mathbf{x})\right]$, respectively. For both cases, the Utopia point can be seen in the last line of Tab. 3.

Once the eigenvectors of the principal components (Tab. 5) show a highly positive relation between PC_1 and R_a, R_y, R_z, R_q and R_t, the minimization of first principal component (PC_1) is justified. On the other hand, there is a strong and positive relation between the first principal component (PC_2) and MRR, which suggest that PC_2 should be maximized.

4.2.4. Payoff matrix calculation and scalarization for NBI matrix

Taking the values of Utopia Point $f_i^U = PC^I{}_i(\mathbf{x})$ and Nadir Point $f_i^N = PC^{Max}{}_i(\mathbf{x})$ developed in previous Step, the Payoff matrix $\overline{\mathbf{\Phi}}$ was developed according to Equation (6). With the values of Payoff matrix, its scalarization was obtained, as Equation (7).

$$\Phi = \begin{bmatrix} -6.201 & 1.576 \\ 0.191 & 2.347 \end{bmatrix} \tag{6}$$

$$\bar{f}(x) = \frac{f_i(x) - f_i^U}{f_i^N - f_i^U} \Rightarrow \begin{Bmatrix} \overline{f_1}(x) = \overline{PC_1}(x) = \dfrac{PC_1(x) - PC_1^{\ I}}{PC_1^{\ Max} - PC_1^{\ I}} \\ \overline{f}_2(x) = \overline{PC_2}(x) = \dfrac{PC_2(x) - PC_2^{\ I}}{PC_2^{\ Max} - PC_2^{\ I}} \end{Bmatrix} \tag{7}$$

$$\bar{f}(x) = \frac{f_i(x) - f_i^I}{f_i^{Max} - f_i^I} \Rightarrow \begin{Bmatrix} \overline{f_1}(x) = \overline{PC_1}(x) = \dfrac{PC_1(x) - PC_1^{\ I}}{PC_1^{\ Max} - PC_1^{\ I}} \\ \overline{f}_2(x) = \overline{PC_2}(x) = \dfrac{PC_2(x) - PC_2^{\ I}}{PC_2^{\ Max} - PC_2^{\ I}} \end{Bmatrix}$$

4.2.5. Run multi-objective nonlinear optimization and Generate Pareto-frontier

Finally, employing the Generalized Reduced Gradient (GRG) algorithm available from Microsoft Excel's Solver® routine for the system of equation (8), the optimization of the values of PC_1 and PC_2 through NBI-PCA approach produced roughness values and MRR. These are shown in Tab. 6.

$$\begin{aligned} &Min \ \ \bar{f}_1(\mathbf{x}) = \left(\frac{PC_1(\mathbf{x}) - PC_1^I(\mathbf{x})}{PC_1^{\max}(\mathbf{x}) - PC_1^I(\mathbf{x})} \right) \\ &s.t.: \ g_1(\mathbf{x}) = \left(\frac{PC_1(\mathbf{x}) - PC_1^I(\mathbf{x})}{PC_1^{\max}(\mathbf{x}) - PC_1^I(\mathbf{x})} \right) - \left(\frac{PC_2(\mathbf{x}) - PC_2^I(\mathbf{x})}{PC_2^{\max}(\mathbf{x}) - PC_2^I(\mathbf{x})} \right) + 2w - 1 = 0 \\ &g_2(\mathbf{x}) = \mathbf{x}^{\mathbf{T}}\mathbf{x} \leq 4 \end{aligned} \tag{8}$$

The nonlinear constraint $\mathbf{x}^{\mathbf{T}}\mathbf{x} \leq 4$ was considered since the axial distance (ρ) is two. Increments of approximately 5% were adopted in the weight (w) distribution. Furthermore, $PC_1(x)$ and $PC_2(x)$ are significant principal components.

Table 6. Optimization results with NBI-PCA approach.

w	Uncoded parameters				Uncoded responses						PC1	PC2	
	f_z	a_p	V_c	a_e	R_a	R_y	R_z	R_q	R_t	MRR			SLS
0	0.207	1.733	324.325	16.886	1.508	8.019	7.012	1.832	8.105	6.046	1,426	-0,618	65,72
0.05	0.193	1.799	324.636	16.666	1.437	7.582	6.605	1.734	7.667	5.796	-2,146	0,340	55,41
0.1	0.183	1.833	325.124	16.534	1.387	7.251	6.315	1.667	7.336	5.546	2,997	1,019	47,75
0.15	0.174	1.853	325.637	16.436	1.345	6.958	6.067	1.610	7.045	5.296	-2,193	-0,496	41,38
0.2	0.165	1.865	326.139	16.362	1.307	6.685	5.843	1.558	6.773	5.045	2,783	-0,705	35,85
0.25	0.157	1.871	326.643	16.301	1.270	6.424	5.632	1.508	6.515	4.794	-2,091	0,651	30,98
0.3	0.149	1.872	327.121	16.253	1.233	6.171	5.430	1.460	6.263	4.542	2,460	1,830	26,64
0.35	0.142	1.868	327.583	16.215	1.196	5.923	5.233	1.412	6.016	4.290	-6,517	0,348	22,77
0.4	0.134	1.860	328.033	16.186	1.158	5.678	5.038	1.364	5.772	4.036	3,191	0,672	19,31
0.45	0.127	1.848	328.459	16.164	1.119	5.433	4.845	1.315	5.528	3.783	-0,547	-1,402	16,24
0.5	0.120	1.832	328.860	16.150	1.078	5.188	4.650	1.265	5.284	3.528	-1,034	1,854	13,53
0.55	0.112	1.811	329.242	16.143	1.035	4.942	4.453	1.212	5.038	3.272	0,236	-0,416	11,16
0.6	0.105	1.785	329.607	16.142	0.990	4.694	4.252	1.157	4.789	3.016	0,708	0,142	9,11
0.65	0.098	1.754	329.979	16.154	0.941	4.442	4.046	1.099	4.537	2.758	0,082	-0,464	7,38
0.7	0.090	1.717	330.205	16.166	0.889	4.186	3.832	1.037	4.278	2.499	0,611	0,229	5,96
0.75	0.083	1.671	330.408	16.191	0.833	3.925	3.608	0.971	4.014	2.239	0,217	-0,089	4,02
0.8	0.076	1.616	330.537	16.227	0.771	3.659	3.372	0.899	3.743	1.976	0,623	-0,199	4,84
0.85	0.068	1.546	330.516	16.277	0.703	3.387	3.122	0.820	3.465	1.711	0,769	-0,245	3,50
0.9	**0.061**	**1.454**	**330.249**	**16.332**	**0.627**	**3.113**	**2.853**	**0.733**	**3.181**	**1.443**	**0,451**	**-0,135**	**3,29**
0.95	0.054	1.322	329.349	16.402	0.544	2.853	2.566	0.636	2.903	1.169	0,516	-0,168	3,38
1	0.050	1.073	327.113	16.390	0.473	2.729	2.326	0.553	2.744	0.887	0,486	-0,156	3,85

Note: The values in bold represent the optimal values obtained by global optimization SLS.

Those 21 Pareto-optimal solutions obtained by NBI-PCA approach is used to build the Pareto-frontier with NBI-PCA method (Fig. 5).

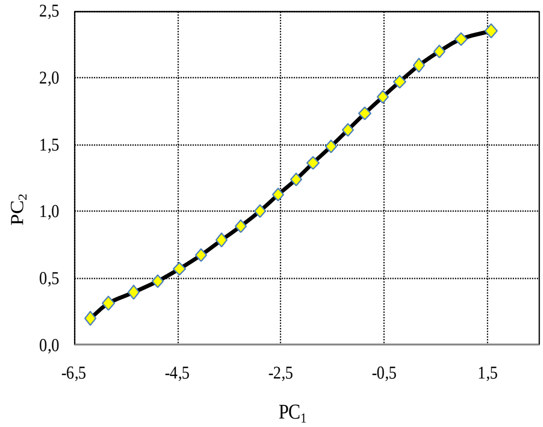

Figure 5. Pareto-frontier obtained with NBI-PCA approach.

Note that the NBI-PCA approach performs an equispaced frontier, avoiding the agglomeration of optimum points in a portion of extreme curvature in the solution space for $-6.134 \leq PC_1 \geq 0.393$ and $0.239 \leq PC_1 \geq 2.156$.

4. 3 Global optimization

To identify the optimal point, the Semiparametric Least Squares (SLS) method, according to the equation (9), was applied on the set of 21 Pareto-optimal solutions obtained by NBI-PCA approach. The goal of the SLS method is find values of $\hat{y}_{ij}$ and ζ_{yi} that minimize the error. The results were already presented in Tab. 6.

$$SLS = \sum_{i=1}^{N}(\hat{y}_{ij} - \zeta_{yi})^2 \text{ , } i = 1,2,\ldots, p \tag{9}$$

Where, $\hat{y}_{ij}$ are the 21Pareto-optimal solutions obtained by multi-objective optimization according the NBI-PCA approach. ζ_{yi} were the Utopia point of surface response.

According the results presented in Tab. 6, the values to maximize the material removal rate while minimizing surface quality simultaneously are f_z = 0.06 mm/tooth, a_p = 1.45 mm, V_c = 330.20 m/min and a_e = 16.33 mm. That is, these were the values that attained the desired quality conditions using the NBI-PCA approach.

Although feed rate (f_z) and axial depth of cut (a_p) have shown values above specification limits, the solution found by NBI-PCA approach was characterized as appropriate optimal point. Furthermore, all the responses optimized by NBI-PCA have been established relatively closer to their Utopia points.

5. CONCLUSION

In this work, an application of NBI with PCA in dry end milling process of AISI 1045 steel was developed. It was possible to reach some conclusions:

The NBI-PCA approach was able to display a uniform pareto-frontier.

The numerical results indicate that the solution found by NBI-PCA approach was characterized as appropriate optimal point.

Material removal rate is maximum and roughness responses are minimum, at f_z = 0.08 mm/tooth, a_p = 1.67 mm, V_c = 330.40 m/min and a_e = 16.19 mm.

The proposed approach shall provide a great assistance to engineers to identify a set of optimal solutions that matches the needs of the organization.

6. ACKNOWLEDGMENTS

To Fapemig, Capes and CNPq.

7. REFERENCES

Antony J. Multi-response optimization in industrial experiments using Taguchi's quality loss function and principal component analysis. *Qual Reliab Eng Int* 2000; 16: 3–8.

Bhogal SS, Sindhu C, Dhami SS, et al. Minimization of Surface Roughness and Tool Vibration in CNC Milling Operation. *J Optim* 2015; 2015.

Bratchell N. Multivariate response surface modelling by principal components analysis. *J Chemom* 1989; 3: 579–588.

Chiao C-H, Hamada M. Analyzing Experiments with Correlated Multiple Responses. *J Qual Technol* 2011; 33: 451–465.

Chen X, Jin Z, Lin G, et al. A novel stereo-model retrieval method in manufacturing. *Proc Inst Mech Eng Part B J Eng Manuf*; 229: 189–198, http://pib.sagepub.com/lookup/doi/10.1177/0954405414564233 (2015).

Das I, Dennis JE. Normal-Boundary Intersection: A New Method for Generating the Pareto Surface in Nonlinear Multicriteria Optimization Problems. *SIAM J Optim* 1998; 8: 631–657.

De Freitas Gomes JH, Júnior ARS, De Paiva AP, et al. Global Criterion Method based on principal components to the optimization of manufacturing processes with multiple responses. *Stroj Vestnik/Journal Mech Eng* 2012; 58: 345–353.

Johnosn R a., Wichern DW. Applied Multivariate Statistical Analysis. 2007.

Kumar MC ---VS---RG---S. To Estimate The Range Of Process Parameters For Optimization Of Surface Roughness & Material Removal Rate In CNC Milling. *Int J Eng Trends Technol* 2013; 4: 4556–4563.

Kumar G, Davis R, Introduction I. OPEN ACCESS A Comparative Analysis of Surface Roughness and Material Removal Rate in Milling Operation of AISI 410 Steel And Aluminium 6061. 2014; 4: 89–93.

Moshat S, Datta S, Bandyopadhyay a, et al. Parametric optimization of CNC end milling using entropy measurement technique combined with grey-Taguchi method. *Int J Eng Sci Technol* 2010; 2: 1–12.

Murthy KS, Rajendran I. Optimization of End Milling Parameters under Minimum Quantity Lubrication Using Principal Component Analysis and Grey Relational Analysis. *J Brazilian Soc Mech Sci Eng* 2012; 34: 253–261.

Paiva AP, Ferreira JR, Balestrassi PP. A multivariate hybrid approach applied to AISI 52100 hardened steel turning optimization. *J Mater Process Technol* 2007; 189: 26–35.

Paiva AP, Costa SC, Paiva EJ, et al. Multi-objective optimization of pulsed gas metal arc welding process based on weighted principal component scores. *Int J Adv Manuf Technol* 2010; 50: 113–125.

Patwari AU. Modeling and Optimization of Tool Life and Surface Roughness for End Milling Titanium Alloy Ti – 6Al – 4V Using Uncoated WC-Co Inserts. 2008; 24–27.

Singh C. Empirical Modeling of Surface Roughness and Metal Removal Rate in CNC Milling Operation. 2014; 1120–1126.

Singh B, Khanna R, Goyal K, et al. Optimization of Input Process Parameters in CNC Milling Machine of EN24 Steel. 2014; 5762: 40–47.

Thangarasu VS, Devaraj G, Sivasubramanian R. High speed CNC machining of AISI 304 stainlesssteel ; Optimization of process parameters by MOGA. *Int J Eng Sci Technol* 2012; 4: 66–77.

Tong L-I, Wang C-H, Chen H-C. Optimization of multiple responses using principal component analysis and technique for order preference by similarity to ideal solution. *Int J Adv Manuf Technol* 2005; 27: 407–414.

Wu F-C. Optimization of Correlated Multiple Quality Characteristics Using Desirability Function. *Qual Eng* 2005; 17: 119–126.

8. AUTHOR RESPONSBILITY

"The authors are the only responsible for the content of this work".